

Effect of local charge fluctuations on spin physics in the Néel state of La_2CuO_4

Luca Capriotti,¹ Andreas Läuchli,² and Arun Paramekanti³

¹*Credit Suisse First Boston (Europe) Ltd., One Cabot Square, London E14 4QJ, United Kingdom*

²*Institut Romand de Recherche Numérique en Physique des Matériaux (IRRMA), PPH-Ecublens, CH-1015 Lausanne*

³*Department of Physics, University of California, Berkeley 94720-7300, U.S.A.*

We explore the effect of local charge fluctuations on the spin response of a Mott insulator by deriving an effective spin model, and studying it using Schwinger boson mean field theory. Applying this to La_2CuO_4 , we show that an accurate fit to the magnon dispersion relation, measured by Coldea *et al.* [Phys. Rev. Lett. **86**, 5377 (2001)] is obtained with Hubbard model parameters $U \approx 2.34\text{eV}$, and $t \approx 360\text{meV}$. These parameters lead to estimates of the staggered magnetization ($m_s \approx 0.25$), spin wave velocity ($c \approx 800\text{meV}\text{-\AA}$), and spin stiffness ($\rho_s \approx 24\text{meV}$). In particular the staggered moment as well as the effective local moment are renormalized to smaller values compared to the Heisenberg model due to local charge fluctuations in the Hubbard model. The dynamical structure factor shows considerable weight in the continuum along the zone boundary as well as secondary peaks that may be observed in high resolution neutron scattering experiments.

PACS numbers:

I. INTRODUCTION

Multispin interactions are important in a variety of magnetic systems.¹ In a magnetically ordered insulator, such interactions can reveal themselves through their effect on the spin dynamics measured in neutron scattering experiments. One system which appears to provide an example of such physics is La_2CuO_4 , which is a Mott insulating antiferromagnet. Indeed, high resolution data on the magnon dispersion in this system indicate a dip in the magnon energy near $\mathbf{Q} = (\pi/2, \pi/2)$ while traversing the magnetic Brillouin zone boundary along $(\pi, 0) \rightarrow (0, \pi)$. Such a dip is not expected for the magnon dispersion in a nearest-neighbor Heisenberg antiferromagnet, but it has been suggested² that this could arise from four-spin interactions generated by local charge fluctuations in the insulating phase. Motivated by this, we revisit the zero temperature Néel ordered state of La_2CuO_4 , and examine how the spin stiffness, the ordered moment, the effective local moment at a site, and the spin dynamics are influenced by local charge fluctuations in this Mott insulator.

La_2CuO_4 is a layered antiferromagnet. While the exchange coupling between the two-dimensional layers is crucial for the existence of a finite-temperature Néel transition in this system, this interplane coupling is nevertheless tiny in magnitude, $\sim 10^{-5}$ of the in-plane exchange coupling, and much smaller than the resolution of the neutron scattering experiments. It is therefore expected that the low temperature spin dynamics in the Néel ordered state in this material is adequately captured by the Hubbard model at zero temperature on a two dimensional square lattice, (with standard notations)

$$H = -t \sum_{\langle ij \rangle, \sigma} \left(c_{i\sigma}^\dagger c_{j\sigma} + h.c. \right) + U \sum_i n_{i\uparrow} n_{i\downarrow} \quad (1)$$

in its insulating phase at strong coupling $U \gg t$. In this regime, it is well known^{3,4} that the low energy physics can

be encapsulated in an effective spin Hamiltonian which incorporates two-spin and four-spin interactions (given below in Eq. 2).

A detailed analysis of a spin model with such four-spin interactions was carried out by Katanin and Kampf⁵ using modified spin wave theory. This allowed them to conclude that a fit to the magnon dispersion indeed requires sizeable four-spin interactions, as originally suggested by Coldea *et al.*² based on linear spin wave theory. A different approach to this problem was adopted by Singh and Goswami⁶ and Peres and Araújo⁷ who used the random-phase approximation (RPA) for the Hubbard model with a spin density wave ground state. This is presumably a better approximation at weak coupling but nevertheless also reproduces the dip in the magnon dispersion near $(\pi/2, \pi/2)$ at intermediate values of U/t .

In this paper, we use Schwinger boson mean field theory to study the magnon dispersion and scattering continuum for the effective spin model in Eq. (2). There are several reasons to try this route. First, in contrast to the RPA studies, this approach of mapping to an effective spin model is explicitly geared towards addressing the strong coupling limit $U/t \gg 1$. It is therefore interesting to compare the two approximations at the intermediate coupling values of experimental interest, especially taking into account modifications to the spin operator which result when going from the Hubbard electronic description to an effective spin model. Indeed, it is satisfying that some of the results obtained here are consistent with the spin-density wave approach for intermediate U/t . Second, Schwinger boson mean field theory is known to work well for the square lattice Heisenberg model and it is worth asking if it continues to be reliable once sizeable four-spin interactions are included, and how such interactions affect the ground state properties and the magnon dispersion. Finally, we consider the scattering continuum beyond the magnon peak in La_2CuO_4 which has not been addressed sufficiently in these earlier papers. (While this

paper was being refereed, a closely related work⁸ which discusses the sum-rule and other issues with neutron scattering experiments in La_2CuO_4 was submitted for publication. We have therefore added a brief discussion of sum-rules within our approach, and refer the reader to the above paper for a detailed analysis of sum rules, the current status of neutron scattering experiments and alternative theoretical approaches to spin dynamics in this system.)

A summary of our main new results is given below.

(i) Comparing the mean field theory results for the ground state energy and static spin structure factor with exact diagonalization studies on small clusters, we show that the mean field theory provides a good description of the ground state of the spin model (2), in the experimentally relevant regime.

(ii) We show that the experimental magnon dispersion is well reproduced by our approach for Hubbard model parameters $U \approx 2.34\text{eV}$, and $t \approx 360\text{meV}$. These parameter values are in reasonable agreement with the experimental estimates⁹ of U , and electronic structure calculations¹⁰ for t . Our estimated ratio $U/t \approx 6.5$ is in rough agreement with the value inferred from RPA calculations for the Hubbard model^{6,7} as well as the quantum Monte Carlo (QMC) calculations of Sengupta *et al.*,¹¹ though we do not resort to the single mode approximation used by the latter authors. It is however slightly smaller than the ratio $U/t \approx 8.8$ obtained from a recent series expansion study of the Hubbard model¹².

(iii) Our best fit parameters for t, U lead to values for the staggered magnetization $m_s \approx 0.25$, spin wave velocity $c \approx 800\text{meV}\text{-\AA}$, and spin stiffness $\rho_s \approx 24\text{meV}$. The spin wave velocity and spin stiffness are in good agreement with experimental findings.¹³ The staggered moment is substantially reduced from that of the Heisenberg model due to local charge fluctuations, as was earlier pointed out by Delannoy *et al.*,¹⁴ and it may be worth revisiting this in experiments.

(iv) Turning to the spin excitation spectrum beyond the magnon, we find that there is a broad continuum of excitations at energy scales relevant to neutron scattering experiments. In addition, the spin-flip operator in the Hubbard model induces transitions into the upper Hubbard band which would show up at energies of $\mathcal{O}(U)$. We however restrict attention in this paper to energies well below the Mott gap, where a spin model description is appropriate. In this regime, we find that, along the zone boundary, the spectral weight in the continuum is about 40% of the total spectral weight. This is similar to the large continuum spectral weight inferred from QMC calculations on the Heisenberg model,¹⁵ but we cannot make any quantitative comparisons at this stage. Turning to the spectral lineshape at energy scales relevant to neutron scattering experiments, we find that the dynamical structure factor exhibits secondary peaks within the mean field theory.

(v) The local charge fluctuations in the Hubbard model also lead to a smaller effective local moment. To ob-

tain this effective moment, we consider integrating the dynamical structure factor over energies well below the Mott gap, as relevant for neutron scattering experiments, and then integrating this “low-energy” equal-time structure factor $\tilde{S}_{\text{low}}(\mathbf{q})$ over \mathbf{q} . This leads to the sum-rule $\sum_{\mathbf{q}} \tilde{S}_{\text{low}}(\mathbf{q}) = S_{\text{eff}}(S_{\text{eff}} + 1)$, with $S_{\text{eff}} < S = 1/2$. Our calculation gives $S_{\text{eff}} \simeq 0.39$.

It is possible that all these features could be explored in neutron scattering experiments with higher resolution and intensity in the near future.

II. EFFECTIVE SPIN MODEL

The effective spin model describing the strong coupling regime of the Hubbard model in (1) takes the form

$$H_{\text{spin}} = \frac{1}{2} \sum_{i,j} J(\mathbf{r}_i - \mathbf{r}_j) \vec{S}_i \cdot \vec{S}_j + \sum_{\square} J_{\square} \left[(\vec{S}_1 \cdot \vec{S}_2)(\vec{S}_3 \cdot \vec{S}_4) + (\vec{S}_1 \cdot \vec{S}_4)(\vec{S}_2 \cdot \vec{S}_3) - (\vec{S}_1 \cdot \vec{S}_3)(\vec{S}_2 \cdot \vec{S}_4) \right]. \quad (2)$$

Here, \vec{S}_i are spin-half operators, and J_{\square} refers to an elementary plaquette on the square lattice with 1 – 4 labeling sites on its corners. The explicit expressions for the exchange couplings in terms of the Hubbard model parameters are⁴,

$$J_1 = J_{\hat{x}} = J_{\hat{y}} = 4 \frac{t^2}{U} - 24 \frac{t^4}{U^3} \quad (3)$$

$$J_2 = J_{\hat{x}+\hat{y}} = J_{\hat{x}-\hat{y}} = 4 \frac{t^4}{U^3} \quad (4)$$

$$J_3 = J_{2\hat{x}} = J_{2\hat{y}} = 4 \frac{t^4}{U^3} \quad (5)$$

$$J_{\square} = 80 \frac{t^4}{U^3} \quad (6)$$

With hopping matrix elements between further neighbor sites in the Hubbard model, we expect additional couplings in the effective spin Hamiltonian. However, electronic structure calculations¹⁰ suggest that these matrix elements are small in magnitude for La_2CuO_4 , so we will not consider them here.

III. SCHWINGER BOSON MEAN FIELD THEORY

To study the ground state and excitations of H_{spin} , we follow Ref. 16 and represent spins using two species of bosons $b_{1,2}$ as

$$\vec{S}_i = b_{i\alpha}^{\dagger} \vec{\sigma}_{\alpha\beta} b_{i\beta} \quad (7)$$

with the constraint

$$b_{i\alpha}^{\dagger} b_{i\alpha} = 2S \quad (8)$$

on the boson number at each site. The $\vec{\sigma}$ are Pauli matrices, the spin $S = 1/2$ for our system and, unless specified, the summation over repeated Greek indices is implied here and below. The Hamiltonian can be reexpressed in terms of the bosons by using the identity

$$\vec{S}_i \cdot \vec{S}_j =: B_{ij}^\dagger B_{ij} : - A_{ij}^\dagger A_{ij}, \quad (9)$$

where $::$ is the standard normal ordering and the bond operators are

$$B_{ij} = \frac{1}{2} b_{i\alpha}^\dagger b_{j\alpha} \quad (10)$$

$$A_{ij} = \frac{1}{2} (b_{i,1} b_{j,2} - b_{i,2} b_{j,1}). \quad (11)$$

In the exact Schwinger boson representation, the Hamiltonian obtained using the above identity consists of 4-boson and 8-boson operators, and one has in addition to deal with the boson number constraint (8). In order to make progress we can resort to a mean field approach. Applied to the Hamiltonian H_{spin} in Eq. (2), this consists of three approximations. (i) First, we reduce the 4-spin interactions to effective 2-spin terms by setting

$$(\vec{S}_1 \cdot \vec{S}_2)(\vec{S}_3 \cdot \vec{S}_4) \rightarrow \langle (\vec{S}_1 \cdot \vec{S}_2) \rangle (\vec{S}_3 \cdot \vec{S}_4) \quad (12)$$

$$+ (\vec{S}_1 \cdot \vec{S}_2) \langle (\vec{S}_3 \cdot \vec{S}_4) \rangle \quad (13)$$

$$- \langle (\vec{S}_1 \cdot \vec{S}_2) \rangle \langle (\vec{S}_3 \cdot \vec{S}_4) \rangle. \quad (14)$$

This renormalizes the two-spin exchange couplings $J(\mathbf{r}_i - \mathbf{r}_j) \rightarrow J^{\text{eff}}(\mathbf{r}_i - \mathbf{r}_j)$ in H_{spin} . It is straightforward to show that $J_1^{\text{eff}} = J_1 + 2J_\square \langle \vec{S}_i \cdot \vec{S}_j \rangle$ where ij are nearest neighbor spins, $J_2^{\text{eff}} = J_2 - J_\square \langle \vec{S}_i \cdot \vec{S}_m \rangle$ where im are next nearest neighbors, and $J_3^{\text{eff}} = J_3$. At this stage, we obtain a Heisenberg spin Hamiltonian $H_{\text{spin}}^{\text{mf}}$ with only two-spin interactions. (ii) Next, we do a mean field decoupling of the 4-boson terms arising from the effective two-spin interactions, setting $: B_{ij}^\dagger B_{ij} : \rightarrow \langle B_{ij}^\dagger \rangle B_{ij} + B_{ij}^\dagger \langle B_{ij} \rangle - \langle B_{ij}^\dagger \rangle \langle B_{ij} \rangle$ and similarly for $A_{ij}^\dagger A_{ij}$. This reduces the spin Hamiltonian $H_{\text{spin}}^{\text{mf}}$ to a quadratic boson Hamiltonian, which up to overall constant terms is given by

$$H_{\text{boson}}^{\text{eff}} = \frac{1}{2} \sum_{i,j} J^{\text{eff}}(\mathbf{r}_i - \mathbf{r}_j) \left[\langle B_{ij}^\dagger \rangle B_{ij} + B_{ij}^\dagger \langle B_{ij} \rangle - \langle A_{ij}^\dagger \rangle A_{ij} - A_{ij}^\dagger \langle A_{ij} \rangle \right] \quad (15)$$

(iii) Finally, we take the constraint (8) into account using a site-independent Lagrange multiplier λ , thus working with the Hamiltonian $H_{\text{boson}}^{\text{mf}} = H_{\text{boson}}^{\text{eff}} - \lambda \sum_i (b_{i\alpha}^\dagger b_{i\alpha} - 2S)$. The Hamiltonian $H_{\text{boson}}^{\text{mf}}$ is readily diagonalized by a Bogoliubov rotation

$$b_{\mathbf{k},1} = u_{\mathbf{k}} f_{\mathbf{k}\uparrow} - v_{\mathbf{k}} f_{-\mathbf{k}\downarrow}^\dagger \quad (16)$$

$$b_{-\mathbf{k},2}^\dagger = -v_{\mathbf{k}}^* f_{\mathbf{k}\uparrow} + u_{\mathbf{k}}^* f_{-\mathbf{k}\downarrow}^\dagger. \quad (17)$$

Defining

$$\beta_{\mathbf{k}} = \sum_{\mathbf{r}} J^{\text{eff}}(\mathbf{r}) B(\mathbf{r}) \cos(\mathbf{k} \cdot \mathbf{r}) \quad (18)$$

$$\alpha_{\mathbf{k}} = \sum_{\mathbf{r}} J^{\text{eff}}(\mathbf{r}) A(\mathbf{r}) e^{-i\mathbf{k} \cdot \mathbf{r}} \quad (19)$$

$$A(\mathbf{k}) = \sum_{\mathbf{r}} A(\mathbf{r}) e^{i\mathbf{k} \cdot \mathbf{r}} \quad (20)$$

$$B(\mathbf{k}) = \sum_{\mathbf{r}} B(\mathbf{r}) e^{i\mathbf{k} \cdot \mathbf{r}}, \quad (21)$$

and choosing

$$\Omega_{\mathbf{k}} = \sqrt{|\beta_{\mathbf{k}} - \lambda|^2 - |\alpha_{\mathbf{k}}|^2} \quad (22)$$

$$u_{\mathbf{k}} = \cosh(\theta_{\mathbf{k}}) e^{-i\gamma_{\mathbf{k}}} \quad (23)$$

$$v_{\mathbf{k}} = \sinh(\theta_{\mathbf{k}}) e^{-i\gamma_{\mathbf{k}}} \quad (24)$$

$$\cosh(2\theta_{\mathbf{k}}) = |\beta_{\mathbf{k}} - \lambda| / \Omega_{\mathbf{k}} \quad (25)$$

$$\sinh(2\theta_{\mathbf{k}}) = |\alpha_{\mathbf{k}}| / \Omega_{\mathbf{k}}. \quad (26)$$

we arrive at the diagonal form

$$H_{\text{boson}}^{\text{mf}} = \frac{1}{2} \sum_{\mathbf{k}, \mu} \Omega_{\mathbf{k}} f_{\mathbf{k}, \mu}^\dagger f_{\mathbf{k}, \mu} + \lambda(S + 1/2) N_{\text{site}} - \frac{1}{2} \sum_{\mathbf{k}} \beta(\mathbf{k}) + \frac{1}{2} \sum_{\mathbf{k}} (A^*(\mathbf{k}) \alpha_{\mathbf{k}} - B^*(\mathbf{k}) \beta_{\mathbf{k}}) \quad (27)$$

The f -particles appearing here are bosonic $S = 1/2$ spinons. The above parameters $u_{\mathbf{k}}, v_{\mathbf{k}}$ depend on the mean field values of $\langle B_{ij} \rangle \equiv B(\mathbf{r})$, $\langle A_{ij} \rangle \equiv A(\mathbf{r})$, and $\langle \vec{S}_i \cdot \vec{S}_j \rangle$ appearing in the quadratic Hamiltonian. These mean field parameters are evaluated in the ground state of (27), which results in a self-consistent theory. For completeness, the self consistency conditions and the constraint equation are given by

$$A(\mathbf{k}) = \frac{\alpha(\mathbf{k})}{2\Omega_{\mathbf{k}}} \quad (28)$$

$$B(\mathbf{k}) = \frac{\beta_{\mathbf{k}} - \lambda}{2\Omega_{\mathbf{k}}} - \frac{1}{2} \quad (29)$$

$$2S + 1 = \frac{1}{N_{\text{site}}} \sum_{\mathbf{k}} \frac{\beta_{\mathbf{k}} - \lambda}{\Omega_{\mathbf{k}}} \quad (30)$$

It is well known¹⁶ that long-range magnetic order appears in this formulation if the energy $\Omega_{\mathbf{k}, \mu}$ vanishes at some wavevector(s) $\mathbf{k} = \{\mathbf{Q}_i\}$ in the thermodynamic limit, leading to condensation of the spinons at these momenta. In the Néel state on the square lattice, the spinons condense at wavevectors $\mathbf{Q} = \pm(\pi/2, \pi/2)$ in the thermodynamic limit¹⁷ leading to magnetic order at the wavevector connecting these points, namely (π, π) . We report below the ground state properties of the model with four-spin interactions, and present a comparison with exact diagonalization results on small clusters.

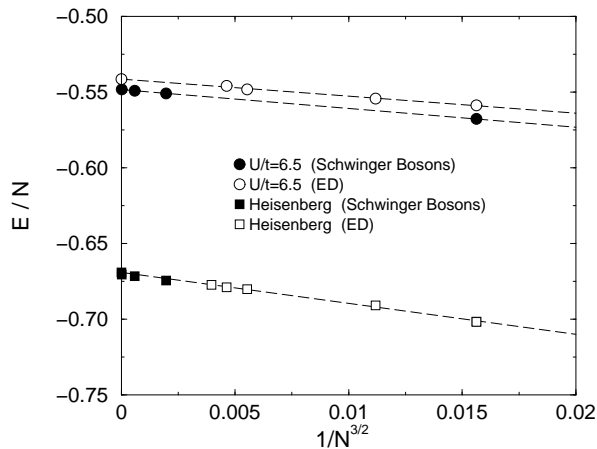


FIG. 1: Comparison of Schwinger boson mean field theory and exact diagonalization calculations of the ground state energy per site for the spin model in Eq. (2) for the Heisenberg limit ($U/t \rightarrow \infty$) and for $U/t = 6.5$.

IV. GROUND STATE PROPERTIES

A. Comparison with exact diagonalization results on small clusters

Schwinger boson mean field theory provides very accurate results for the ground state properties of the nearest-neighbor Heisenberg antiferromagnet¹⁶. In order to assess the accuracy of this approximation scheme in presence of the four-spin interaction term it is useful to compare the mean-field estimates of ground state properties with exact diagonalization numerics. To this end, we have performed Lanczos exact diagonalizations of the spin Hamiltonian (2) on the 4×4 , $\sqrt{20} \times \sqrt{20}$, $\sqrt{32} \times \sqrt{32}$ and 6×6 clusters. In particular we have focused on exchange interactions corresponding to $U/t \rightarrow \infty$ (the Heisenberg limit), and $U/t = 6.5$, for which the mean field theory fits the experimental magnon dispersion of La_2CuO_4 as discussed in the next section. The latter choice of U/t corresponds to $J_2 = J_3 = 0.0276J_1$ and $J_\square = 0.55J_1$ in (2).

We have calculated the ground state energy and the static spin structure factor $S(\mathbf{q})$

$$S(\mathbf{q}) = \sum_j \langle \vec{S}(\mathbf{r}_j) \cdot \vec{S}(\mathbf{r}_0) \rangle e^{-i\mathbf{q} \cdot (\mathbf{r}_j - \mathbf{r}_0)} \quad (31)$$

The results presented in Figs. 1 and 2 clearly show that the Schwinger boson approach is still rather accurate even for large four-spin interactions which are generated for a moderate interaction strength $U/t = 6.5$. We next turn to the staggered magnetization and spin stiffness in the thermodynamic limit for this parameter value, taking into account the modification of the spin operator by local charge fluctuations.

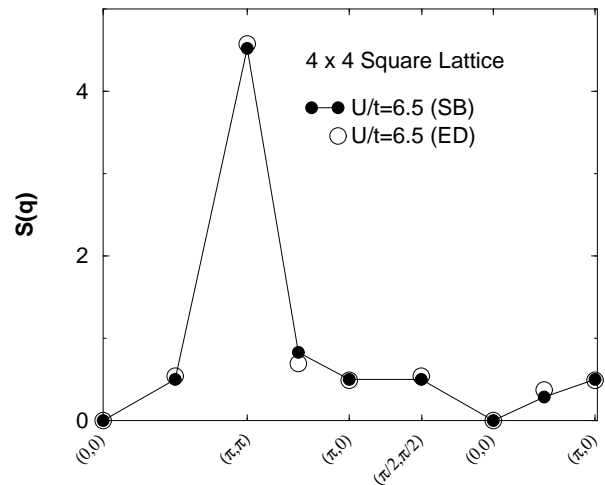


FIG. 2: Comparison of Schwinger boson mean field theory and exact diagonalization calculations of the static (equal-time) spin structure factor $S(\mathbf{q})$ on a 4×4 lattice. These results are for the bare spin-spin correlation function, where the transformation of the spin operator in going from the Hubbard model to the spin model have not been included — including them modifies the mean-field and the exact diagonalization results in the same manner, as discussed in the text, and does not affect our comparison.

B. Staggered magnetization and spin stiffness in the thermodynamic limit

As mentioned earlier, the local charge fluctuations in the Hubbard model affect the spin correlations. We can take this into account by noticing that the spin operator of the Hubbard model is modified by the same unitary transformation which enables us to rotate from the Hubbard model Hamiltonian to the Heisenberg model with four-spin interactions of Eq. (2) which has no charge fluctuations. This transformation was discussed earlier in the context of various physical correlations in the doped cuprate superconductors¹⁸, and its importance for spin physics in the undoped Mott insulator was pointed out by Delannoy *et al.*¹⁴

For instance, making the unitary transformation on the spin operator $S^+(\mathbf{r})$, we find

$$\begin{aligned} \tilde{S}^+(\mathbf{r}) = & S^+(\mathbf{r}) \left(1 - 4 \frac{t^2}{U^2} \right) + \frac{t^2}{U^2} \sum_{\alpha=\pm\hat{x},\pm\hat{y}} S^+(\mathbf{r} + \alpha) \\ & - \frac{t}{U} \sum_{\alpha=\pm\hat{x},\pm\hat{y}} \left(c_{\mathbf{r}+\alpha,\uparrow}^\dagger c_{\mathbf{r},\downarrow} - c_{\mathbf{r},\uparrow}^\dagger c_{\mathbf{r}+\alpha,\downarrow} \right) \quad (32) \end{aligned}$$

While the first two terms lead to spin flips within the lower Hubbard band, the last term excites an electron into the upper Hubbard band. This final term plays a role at high energies, of $\mathcal{O}(U)$, and short distances¹⁹. We will therefore not consider it below, but restrict attention to energies well below the Mott gap, where the first

two terms alone play a role and our spin-only description is valid. With this caveat, we find at $\mathcal{O}(t/U)^2$ we find that the transformed “low energy” equal-time spin-spin correlation function is given by

$$\begin{aligned} \tilde{\mathcal{S}}_{\text{low}}(\mathbf{r} - \mathbf{r}') &= \langle \vec{S}(\mathbf{r}) \cdot \vec{S}(\mathbf{r}') \rangle (1 - 8 \frac{t^2}{U^2}) \\ &+ \frac{t^2}{U^2} \sum_{\alpha=\pm\hat{x},\pm\hat{y}} \langle \vec{S}(\mathbf{r} + \alpha) \cdot \vec{S}(\mathbf{r}') \rangle \\ &+ \langle \vec{S}(\mathbf{r}) \cdot \vec{S}(\mathbf{r}' + \alpha) \rangle \end{aligned} \quad (33)$$

Within Schwinger boson mean field theory, we obtain the antiferromagnetic order parameter m_s from finite-size scaling of the static structure factor, defined via

$$\tilde{\mathcal{S}}_{\text{low}}(\mathbf{q}) = \sum_j \tilde{\mathcal{S}}_{\text{low}}(\mathbf{r}_j - \mathbf{r}_0) e^{-i\mathbf{q} \cdot (\mathbf{r}_j - \mathbf{r}_0)}, \quad (34)$$

as

$$m_s^2 = \lim_{N_{\text{site}} \rightarrow \infty} \frac{\tilde{\mathcal{S}}_{\text{low}}(\pi, \pi)}{N_{\text{site}}}. \quad (35)$$

We find that the staggered magnetization for $U/t = 6.5$ extrapolates to $m_s \approx 0.25$, smaller than that for the nearest-neighbor Heisenberg model ($m_s^{nn} \approx 0.303$). This decrease of the staggered magnetization is due to local charge fluctuations in the insulator, and arises from $\mathcal{O}(t/U)^2$ terms in the modified spin operator in Eq. (32) as pointed out in Ref. 14.

For a pure spin model of the copper sites in La_2CuO_4 , we expect the sum-rule on the equal-time structure factor $\sum_{\mathbf{q}} S(\mathbf{q}) = S(S+1)$ with $S = 1/2$. However, with the above modification to the spin correlations, this sum-rule is corrected by terms of order $(t/U)^2$. Specifically, imagine integrating the dynamical structure factor over energies relevant to neutron scattering experiments, i.e. much smaller than the Mott gap, and then integrating this “low-energy” equal-time structure factor $\tilde{\mathcal{S}}_{\text{low}}(\mathbf{q})$ over all \mathbf{q} . In this case, we find the modified relation $\sum_{\mathbf{q}} \tilde{\mathcal{S}}_{\text{low}}(\mathbf{q}) = S_{\text{eff}}(S_{\text{eff}} + 1)$ with $S_{\text{eff}} \simeq 0.39$. It would be interesting to look for this apparent sum-rule deficit in neutron scattering studies.

Following Stringari²⁰, we extract the spin stiffness from the small momentum behavior of the structure factor. Specifically, approaching the magnetically ordered state in a rotationally invariant formulation, the static structure factor for small q is related to the spin stiffness through

$$\rho_s = \frac{c\tilde{\mathcal{S}}(\mathbf{q} \rightarrow 0)}{q} \quad (36)$$

where c is the spin wave velocity of the linearly dispersing magnon at momenta near $(0,0)$ and (π,π) . The spin-wave velocity c can be obtained from the magnon dispersion as discussed in connection with the excitation spectrum in the next section. This, together with the calculated structure factor in the limit, $\mathbf{q} \rightarrow 0$, yields the

spin stiffness through Eq. (36). As discussed in detail in the next section, a fit to the overall magnon dispersion in La_2CuO_4 yields a spin wave velocity $c \approx 800 \text{meV}\cdot\text{\AA}$. Assuming a lattice spacing 3.85\AA for the CuO_2 plane, this yields $\rho_s \approx 24 \text{meV}$, which is consistent with experimental findings.¹³ Note that the spin stiffness can also be obtained by studying the change in ground state energy for a slowly varying spin twist.

V. EXCITATION SPECTRUM

To probe the spectrum of $S = 1$ excitations at a given momentum \mathbf{q} , which is of interest for neutron scattering experiments, one can act with the operator $S^+(\mathbf{q}) = \sum_{\mathbf{k}} b_{\mathbf{k},1}^\dagger b_{\mathbf{k}-\mathbf{q},2}$ onto the ground state^{20,22}. Making a Bogoliubov rotation to spinon variables, we can rewrite this as

$$\begin{aligned} S^+(\mathbf{q}) &= \sum_{\mathbf{k}} \left(u_{\mathbf{k}} f_{\mathbf{k}\uparrow} - v_{\mathbf{k}} f_{-\mathbf{k}\downarrow}^\dagger \right) \\ &\times \left(u_{\mathbf{k}-\mathbf{q}} f_{\mathbf{k}-\mathbf{q},\uparrow} - v_{\mathbf{k}-\mathbf{q}} f_{-\mathbf{k}+\mathbf{q},\downarrow}^\dagger \right). \end{aligned} \quad (37)$$

Including corrections to the spin operator via the unitary transformation, discussed earlier for the static structure factor, leads to two modifications in the dynamical response. The first is a simple modification of the spin operator by a multiplicative “form factor” $S^+(\mathbf{q}) \rightarrow G(\mathbf{q})S^+(\mathbf{q})$, with

$$G(\mathbf{q}) = 1 - \frac{2t^2}{U^2} (2 - \cos q_x - \cos q_y) \quad (38)$$

This will not affect the magnon energies but will correct the dynamical response by an overall multiplicative prefactor $G^2(\mathbf{q})$.

The second effect of this unitary transformation as discussed is to generate a new term which causes a transition from the lower to the upper Hubbard band. This term plays a role only if we examine spin dynamics at very high energies, and is of no relevance at energies probed in the neutron scattering experiments to which we restrict attention here. We see that at a given momentum \mathbf{q} , if one of the two spinons combining to give the spin operator in Eq. (37) is condensed (which would happen for spinon momenta $\pm(\pi/2, \pi/2)$ in the Néel state), that part behaves as a single particle excitation with a well defined dispersion - this is the magnon. For general \mathbf{k} , both spinons are uncondensed and this remainder of the sum contributes to the scattering continuum. Quite generally, both parts play a role when we evaluate the spectral function for the $S^+(\mathbf{q})$ operator.

A. Magnon dispersion

From the above discussion, it is clear that the magnon energy at momentum \mathbf{q} within the mean field theory

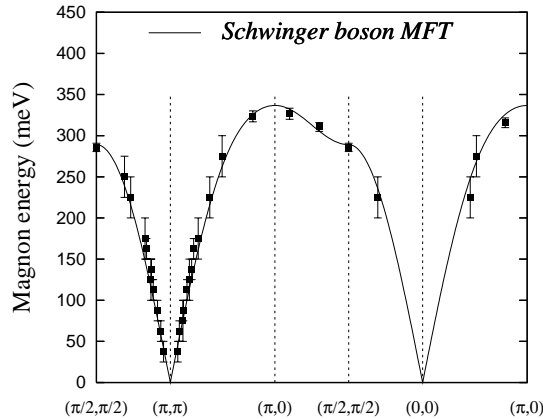


FIG. 3: Fit of the magnon dispersion obtained from Schwinger boson mean field theory to the experimental data at $T = 10K$ in Ref. 2 along the standard contour in the Brillouin zone. The Hubbard model parameters used for this fit are $t = 360meV$ and $U = 2.34eV$, with the effective spin Hamiltonian couplings given by Eq. (6).

of the Néel state is just given by $\Omega_{\mathbf{Q}-\mathbf{q}}/2$ where $\mathbf{Q} = \pm(\pi/2, \pi/2)$. For our choice of mean field decoupling, and for spin $S \rightarrow \infty$, this is exactly half the value given by spin-wave theory²¹. It is known²² that Schwinger boson mean field theory for the Heisenberg model has this shortcoming, which can be fixed by working within a large- N generalization of the Schwinger boson theory and including $1/N$ corrections to the mean field ($N = \infty$) result. Since we reduce our original Hamiltonian in Eq. (2) to an effective Heisenberg-type model before we use the Schwinger boson representation, we expect the same fluctuation corrections to appear in our case as well, however an explicit calculation is beyond the scope of this paper. Here and below we will work with $\Omega_{\mathbf{k}}$ as the magnon energy. Note that the $\mathcal{O}(t/U)^2$ corrections to the spin operator do not affect the magnon dispersion. Fig. 3 shows the magnon energy $\Omega_{\mathbf{k}}$ obtained within the mean field theory for $U/t = 6.5$ and $t = 360meV$ compared with the experimental data from Coldea *et al.* This choice of parameters gives a good fit to the dispersion over the entire contour along the Brillouin zone, including both the linearly dispersing spin-wave regime as well as the high energy magnon dispersion along the zone boundary. While the fit along the zone boundary is easy to see in the figure, its accuracy at low energies may be seen from the spin wave velocity in the mean field theory $c \approx 800meV\text{-}\text{\AA}$ being in good agreement with experiment. We also point out that at much larger values of U/t ($\gtrsim 7$), we are unable to reproduce properly the dip in the magnon dispersion at $(\pi/2, \pi/2)$ while traversing the zone boundary. While further neighbor hoppings in the Hubbard model (e.g. third-nearest neighbor hopping t_3) could produce

a similar dip near $(\pi/2, \pi/2)$ by generating an antiferromagnetic exchange of order t_3^2/U , electronic structure calculations for La_2CuO_4 indicate that such hopping matrix elements are too small to be relevant.

B. Scattering continuum

Having fixed the parameter values U, t from fitting the magnon dispersion to the data, we next turn to the scattering continuum. Specifically, we are interested in asking how much weight is present in the continuum relative to the magnon, and if there are any features in the continuum which may be experimentally observable. Recall that in the mean field theory this part of the spectrum is just the two-spinon excitation continuum. In order to obtain the weight in the continuum versus the magnon, we consider the energy integrated response. This is just the structure factor

$$S(\mathbf{q}) = \sum_{\mathbf{k}} \left[\left(\frac{|\beta_{\mathbf{k}-\mathbf{q}} - \lambda|}{\Omega_{\mathbf{k}-\mathbf{q}}} - 1 \right) \left(\frac{|\beta_{\mathbf{k}} - \lambda|}{\Omega_{\mathbf{k}}} + 1 \right) - \frac{\alpha_{\mathbf{k}}^* \alpha_{\mathbf{k}-\mathbf{q}}}{\Omega_{\mathbf{k}} \Omega_{\mathbf{k}-\mathbf{q}}} \right] \quad (39)$$

To obtain the magnon weight part, we need to keep only those contributions where $\Omega_{\mathbf{k}}$ or $\Omega_{\mathbf{k}-\mathbf{q}}$ would vanish in the thermodynamic limit (or are minimum on a finite but large lattice). The continuum contribution is the remaining part of the sum. Fig. 4 shows the ratio of these weights along the same contour in the Brillouin zone over which the magnon dispersion is displayed. This ratio is clearly insensitive to the “form factor” $G(\mathbf{q})$, however the important thing to note from the plot is that the continuum weight is most significant along the zone boundary and accounts for nearly 40% of the total spectral weight. This is the most promising region to study the continuum in neutron scattering experiments. The continuum weight is also considerable along the line from $(\pi, 0)$ to $(\pi, \pi/2)$. This is qualitatively similar to results inferred for the Heisenberg model from QMC calculations¹⁵. In order to display possible interesting features in the continuum scattering we have plotted the spectrum of excitations at a few \mathbf{q} points along the zone boundary in Fig. 6, as well a grayscale plot of the spectral function in Fig. 5 along $(0, 0) \rightarrow (\pi, \pi)$ and along $(\pi, 0) \rightarrow (0, \pi)$. We see that in addition to the magnon, there are singular secondary features in the spectrum. These secondary peaks can be shown to arise from special points $\{\mathbf{K}\}$ in the Brillouin zone in the vicinity of which the sum $\Omega_{\mathbf{k}} + \Omega_{\mathbf{k}-\mathbf{q}}$ varies slowly (dispersing as $\sim |\mathbf{k} - \mathbf{K}|^4$) giving rise to a log singular density of states for the two-spinon continuum. These secondary peaks and continuum scattering also arise within the mean field theory for the nearest neighbor Heisenberg model, with minor quantitative changes due to differences in the spinon dispersion. The effect of fluctuations beyond the mean field result on the magnon dispersion and the scattering con-

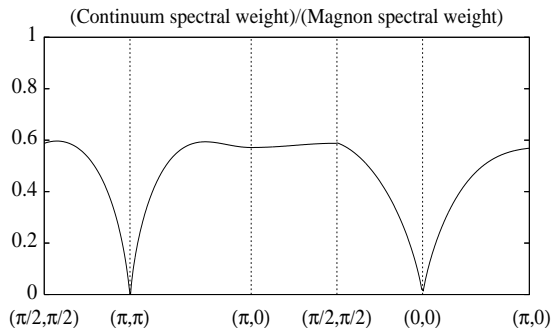


FIG. 4: Ratio of continuum and magnon spectral weights along a contour in the Brillouin zone. The magnon exhausts the spectral weight for $\mathbf{q} \rightarrow (0, 0)$ and $\mathbf{q} \rightarrow (\pi, \pi)$ consistent with general arguments²⁰. Along the zone boundary, the continuum accounts for nearly 40% of the total spectral weight.

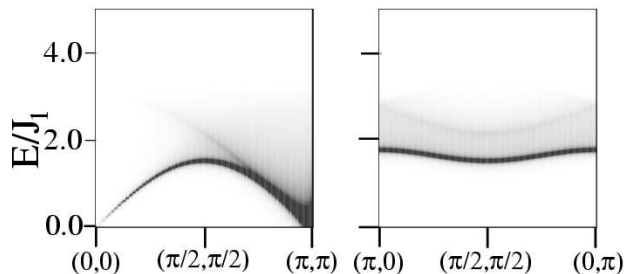


FIG. 5: Grayscale plot of the dynamical structure factor $S(\mathbf{q}, E)$ of the spin model (2) with optimal parameters as in Fig. 1, with high intensity in black. The gray areas indicate regions of continuum scattering. The intensity has been scaled to clearly show both the magnon and secondary peak features. Left panel: Magnon peak and the single secondary peak along $(0, 0) \rightarrow (\pi, \pi)$. The magnon and secondary peak intensities vanish as $\mathbf{q} \rightarrow (0, 0)$. Right panel: Magnon peak and two secondary peaks along the zone boundary $(\pi, 0) \rightarrow (0, \pi)$. The two secondary peaks merge at $(0, \pi)$ and $(\pi, 0)$. The dip in the magnon dispersion at $(\pi/2, \pi/2)$ is clearly visible.

tinuum is beyond the scope of this paper, and is currently being investigated.

VI. CONCLUDING REMARKS

We have presented a Schwinger boson mean-field description of the effect of four-spin interactions on spin dynamics in Mott insulators. Such multispin interactions and their effects are potentially important in any correlated insulator with local charge fluctuations. For La_2CuO_4 , the experimental magnon dispersion is well re-

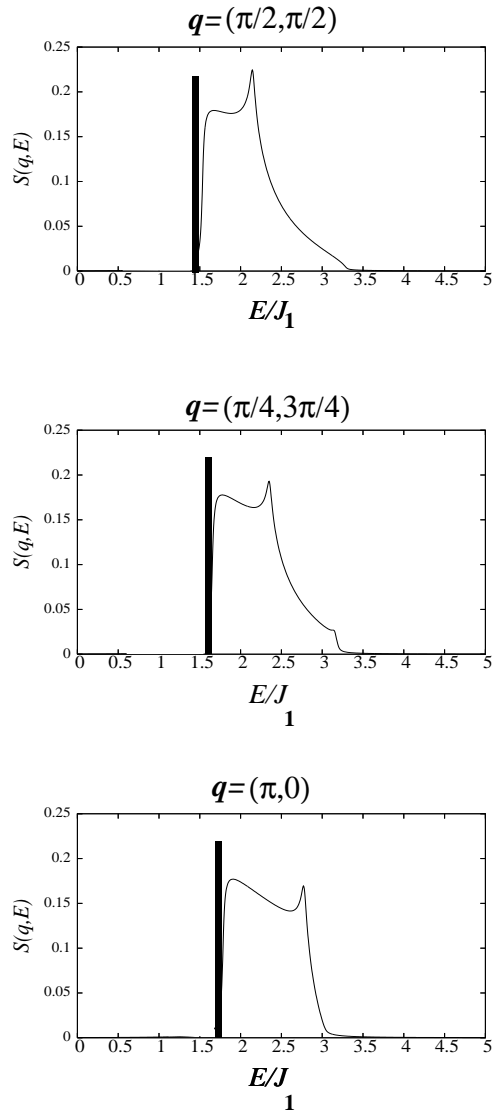


FIG. 6: The dynamical structure factor along the zone boundary at $(\pi/2, \pi/2)$ (top), $(\pi/4, 3\pi/4)$ (middle) and $(\pi, 0)$ (bottom), showing the sharp magnon (as a bold vertical line not drawn to scale) and the broad continuum including the sharp secondary features most clearly visible at $(\pi/4, 3\pi/4)$.

produced by our approach with Hubbard model parameters $U \approx 2.34eV$, and $t \approx 360meV$. These values are consistent with the experimental estimates⁹, and electronic structure calculations¹⁰. This leads to a sizeable value of the four-spin exchange term $J_{\square} \approx 0.55J_1$ in the effective spin Hamiltonian. Good agreement with experiments is also obtained for spin wave velocity and spin stiffness, thus leading to a consistent description of the magnetic behavior of this Mott insulator. The staggered moment is substantially reduced from that for the Heisenberg model, it would be worth revisiting experiments to test for this reduced ordered moment. We have also discussed

differences in sum rules between Hubbard and Heisenberg models, and refer the reader to more recent work⁸ for additional insights, alternative approaches, and the current experimental status. Beyond the single magnon excitation, we have shown that there is considerable spectral weight in the continuum along the zone boundary, and that the dynamical structure factor exhibits secondary peaks which we understand as arising from the density of states of two-spinon excitations. These could be explored in experiments with high intensity neutron sources in the near future.

Acknowledgments

We thank Radu Coldea, Gregoire Misguich and Prof. Andre-Marie Tremblay for very useful discussions and correspondence, and Anton Burkov for an early stimulating conversation. AP acknowledges support through grant DOE LDRD DEAC03-76SF00098. The numerical calculations have been performed on the “Mizar” SMP machine at EPFL.

-
- ¹ D.J. Thouless, Proc. Phys. Soc. (London) **86** 893 (1965); M. Roger, J.H. Hetherington, and J.M. Delrieu, Rev. Mod. Phys. **55** 1 (1983); B. Bernu, L. Candido, and D.M. Ceperley, Phys. Rev. Lett. **86**, 870 (2001); K. Voelker and S. Chakravarty, Phys. Rev. B **64**, 235125 (2001).
- ² R. Coldea, S.M. Hayden, G. Aeppli, T.G. Perring, C.D. Frost, T.E. Mason, S.-W. Cheong, and Z. Fisk, Phys. Rev. Lett. **86**, 5377 (2001).
- ³ M. Takahashi, J. Phys. C **10**, 1289 (1977).
- ⁴ A. H. MacDonald, S. M. Girvin, and D. Yoshioka, Phys. Rev. B **41**, 2565 (1990).
- ⁵ A. Katanin and A. Kampf, Phys. Rev. B **66**, 100403 (2002).
- ⁶ A. Singh and P. Goswami, Phys. Rev. B **66**, 092402 (2002).
- ⁷ N.M.R. Peres and M.A.N. Araújo, Phys. Rev. B **65**, 132404 (2002).
- ⁸ J. Lorenzana, G. Seibold and R. Coldea, cond-mat/0507131 (unpublished).
- ⁹ S.L. Cooper, G.A. Thomas, A.J. Millis, P.E. Sulewski, J. Orenstein, D.H. Rapkine, S.-W. Cheong and P.L. Trevor, Phys. Rev. B **42**, 10785 (1990); Y. Tokura, Y. Koshihara, T. Arima, H. Takagi, S. Ishibashi, T. Ido and S. Uchida, Phys. Rev. B **11657** (1990).
- ¹⁰ E. Pavarini, I. Dasgupta, T. Saha-Dasgupta, O. Jepsen and O.K. Andersen, Phys. Rev. Lett. **87**, 047003 (2001).
- ¹¹ P. Sengupta, R. Scalettar, R.R.P. Singh, Phys. Rev. B **66**, 144420 (2002).
- ¹² W. Zheng, R.R.P. Singh, J. Oitmaa, O.P. Sushkov and C.J. Hamer, Phys. Rev. B **72**, 033107 (2005).
- ¹³ K. Yamada, K. Kakurai, Y. Endoh, T.R. Thurston, M.A. Kastner, R.J. Birgeneau, G. Shirane, Y. Hidaka, and T. Murakami, Phys. Rev. B **40**, 4557 (1989); B. Keimer, N. Belk, R.J. Birgeneau, A. Cassanho, C.Y. Chen, M. Greven, M.A. Kastner, A. Aharony, Y. Endoh, and R.W. Erwin, Phys. Rev. B **46**, 14034 (1992).
- ¹⁴ J.-Y.P. Delannoy, M.J.P. Gingras, P.C.W. Holdsworth and A.-M.S. Tremblay, cond-mat/0412033 (unpublished).
- ¹⁵ A. Sandvik and R.R.P. Singh, Phys. Rev. Lett. **86**, 528 (2001).
- ¹⁶ D.P. Arovas and A. Auerbach, Phys. Rev. B **38**, 316 (1988); S. Sarker, C. Jayaprakash, H.R. Krishnamurthy and M.Ma, Phys. Rev. B **40**, 5028 (1989); H.A. Ceccatto, C.J. Gazza, and A.E. Trumper, Phys. Rev. B **47**, 12329 (1993); for an excellent review see also: G. Misguich, Ph.D. thesis, Université Paris 6 (1999), in French.
- ¹⁷ This is for our particular mean field decoupling. The spinon dispersion is not a gauge invariant quantity, although the number of gapless wavevectors and the momentum difference between them are gauge invariant.
- ¹⁸ A. Paramekanti, M. Randeria and N. Trivedi, Phys. Rev. Lett. **87**, 217002 (2001); A. Paramekanti, M. Randeria and N. Trivedi, Phys. Rev. B **70**, 054504 (2004).
- ¹⁹ This term was inadvertently omitted in the earlier version of this paper, we are indebted to Prof. Andre-Marie Tremblay for pointing this out to us.
- ²⁰ S. Stringari, Phys. Rev. B **49**, 6710 (1994).
- ²¹ P.W. Anderson, Phys. Rev. **86**, 694 (1952).
- ²² See for instance the discussion in A. Auerbach, “*Interacting Electrons and Quantum Magnetism*”, Springer-Verlag (1994). For the mean field decoupling scheme used in this book and in some earlier papers, the mean field theory gets the static structure factor and the correction to the classical ground state energy incorrect by a factor of 3/2 and 2 respectively. By contrast, our mean field decoupling gives accurate ground state properties (structure factor and energy) but a factor-of-two difference appears in the magnon dispersion.